

All-Sky Cosmic-Ray Anisotropy Update at Multiple Energies

The IceCube & HAWC Collaborations

(a complete list of authors can be found at the end of the proceedings)

E-mail: juancarlos@icecube.wisc.edu, rykore@wisc.edu,
paolo.desiati@icecube.wisc.edu, fawolf@wisc.edu

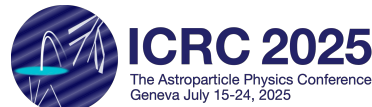
We present preliminary results on an updated full-sky analysis of the cosmic-ray arrival direction distribution with data collected by the High-Altitude Water Cherenkov (HAWC) Observatory and IceCube Neutrino Observatory with complementary field of views covering a large fraction of the sky. This study extends the energy range to higher energies. The HAWC Observatory, located at 19°N has analyzed 8 years of cosmic-ray data over an energy range between 3.0 TeV and 1.0 PeV and confirms an energy-dependent anisotropy in the arrival direction distribution of cosmic rays seen by other experiments. Combined with recently published results from IceCube with 12 years of data, the combined sky maps with 93% coverage of the sky —between 70°N and 90°S— and the corresponding angular power spectra largely eliminate biases that result from partial sky coverage.

Corresponding authors: Juan Carlos Díaz Vélez^{1*}, Riya Yogesh Kore¹, Paolo Desiati¹, Ferris Wolf¹

¹ Dept. of Physics and Wisconsin IceCube Particle Astrophysics Center, University of Wisconsin—Madison, Madison, WI 53706, USA

* Presenter

39th International Cosmic Ray Conference (ICRC2025)
15–24 July 2025
Geneva, Switzerland



1. Introduction

Over the last few decades, several ground-based experiments in both the northern and southern hemispheres have observed variations at the level of 10^{-3} in the arrival direction distribution of cosmic rays with energies between 1 TeV to several PeVs with high statistical accuracy (see [1] and references therein). The limited integrated field of view (FoV) of the sky in all of these individual measurements restricts our ability to characterize the anisotropy in terms of its spherical harmonic components, as large correlations between terms $a_{\ell m}$ bias the interpretation of the cosmic ray distributions [2, 3]. In this analysis, we apply the same methods used in [3] to combine data from the IceCube [4] and HAWC [5] observatories and produce maps with near full-sky coverage to study arrival direction distributions at different energies.

2. Data

The northern hemisphere data used for this analysis were collected by the HAWC gamma-ray Observatory over the span of 8 years from May 2015 to May 2023. The data were split into 11 energy bins. In HAWC, the primary energy was estimated using the logarithm of the number of photomultiplier tubes (PMTs) triggered by each event ($\log_{10} N_{\text{hit}}$), the corresponding reconstructed shower zenith angle ($\cos \theta_{\text{reco}}$), and the radial distance from the center of the HAWC array to the reconstructed shower core location (R_{core}). A four-dimensional histogram including the logarithm of the true primary cosmic-ray energy ($\log_{10} E_{\text{true}}$) is fit with a B-spline function [6], which provides a smooth lookup table for the median energy of cosmic rays in a similar way as in [7]. The IceCube dataset is described in detail in [1], though energy cuts have been adjusted to match the data from comparable HAWC maps as will be discussed in section 5. Table 1 shows the number of events in each of the 11 datasets along with the corresponding median energy and rigidity.

Bin	Rigidity (TV)	HAWC Energy (TeV)	IceCube Energy (TeV)	Events
0	0.6	1.8	–	33.7×10^9
1	1.1	3.2	–	58.0×10^9
2	2.2	5.6	–	44.2×10^9
3	4.1	10.0	–	33.4×10^9
4	7.4	17.8	10.0	3×10^{11}
5	12.5	31.6	14.8	2.9×10^{11}
6	23.2	56.2	30.2	1.1×10^{11}
7	40.0	100.0	53.4	3.2×10^{10}
8	75.5	177.8	310.5	1.9×10^9
9	140.9	316.2	725.3	4.3×10^9
10	280.5	562.3	1716	9.9×10^7

Table 1: Median cosmic-ray primary energy bins used in this analysis, along with corresponding rigidity according to the GST composition model and number of events for each map.

2.1 Surface Pressure and Solar Dipole

Atmospheric conditions, particularly pressure and temperature, can influence cosmic ray detection rates at observatories like HAWC and IceCube. The HAWC Observatory is located below

the shower maximum (X_{\max}) for energies around 10 TeV. As a result, an increase in surface pressure leads to greater atmospheric overburden, attenuating air showers and reducing the event rate. This anti-correlation is quantified with a barometric coefficient, which we have determined experimentally to be $\beta = -0.0086 \text{ hPa}^{-1}$ from local measurements. While many of the pressure variations are due to weather, there is a bi-diurnal variation caused by a tidal effect from solar heating. This variation can introduce a spurious signal in the presence of large time gaps in data taking. The data are weighted to compensate for this effect, leaving minimal residual effects. In contrast, IceCube's muon rate is positively correlated with stratospheric temperature and exhibits strong seasonal variations due to its polar location. Although these atmospheric effects could modulate the Solar dipole signal, their influence is minor in the case of IceCube (see [8] and references therein).

In addition to this spurious signal, the Earth's revolution around the Sun produces a faint Compton-Getting dipole anisotropy [9] with an excess oriented towards the direction of motion in solar coordinates. The relative rotation of the celestial and solar reference frames over a calendar year causes interference between the two sources of anisotropy. This dipole has a predictable phase and amplitude given by

$$\frac{\delta I}{I} = \frac{v(t)}{c} [\gamma(E) + 2] \cos \xi, \quad (1)$$

where I the cosmic ray intensity, $\gamma(E)$ the cosmic-ray spectral index, $v(t)/c$ the ratio of Earth's orbital velocity to the speed of light, and ξ the angle between the cosmic ray particle's arrival direction and the direction of Earth's motion. As with the pressure variations, we can compensate by weighting each event accordingly. The combined weight, with the pressure correction for event i , is given by

$$w_i = e^{-\beta(p(t_i) - p_0)} \left(1 - \frac{v(t_i)}{c} [\gamma(E_i) + 2] \cos \xi_i \right), \quad (2)$$

where $p(t_i)$ is the measured pressure at the time t_i , p_0 is the baseline average pressure over time, $v(t_i)$ corresponds to Earth's orbital speed at time t_i (obtained from the PAL astronomical library [10]) and $\gamma(E_i)$ is the spectral index at energy E_i derived from a fit to the measurement of the all-particle cosmic-ray spectrum by HAWC [11].

3. Relative Intensity

The relative intensity in J2000 equatorial coordinates (α, δ) is obtained by binning the sky into pixels of size 0.9° using the HEALPix library [12]. The residual anisotropy δI of the distribution of arrival directions of the cosmic rays is calculated by subtracting a reference map that describes the detector response to an isotropic flux

$$\delta I_j = \frac{N_j - \langle N_j \rangle}{\langle N_j \rangle}. \quad (3)$$

This relative intensity gives the amplitude of deviations in the number of counts N_j from the isotropic expectation $\langle N_j \rangle$ in each pixel j .

The isotropic expectation $\langle N_j \rangle$ and relative intensity are calculated using a likelihood-based reconstruction method for combined data sets from multiple observatories that have overlapping exposure regions in the sky. The method is described in [13] and does not rely on detector

simulations, providing an optimal anisotropy reconstruction and the recovery of the large-scale anisotropy projected onto the equatorial plane.

4. Statistical Significance

In order to calculate the statistical significance of anisotropy features in the final reconstructed map, we apply a generalized version ([13]) of the Li–Ma method in [14]. The significance map is calculated using

$$S_i = \sqrt{2} \left(-\mu_{i,\text{on}} + \mu_{i,\text{off}} + n_i \log \frac{\mu_{i,\text{on}}}{\mu_{i,\text{off}}} \right)^{1/2}. \quad (4)$$

For each pixel i , we define expected *on-source* and *off-source* event counts from neighbor pixels in a disc of radius r centered on that pixel.

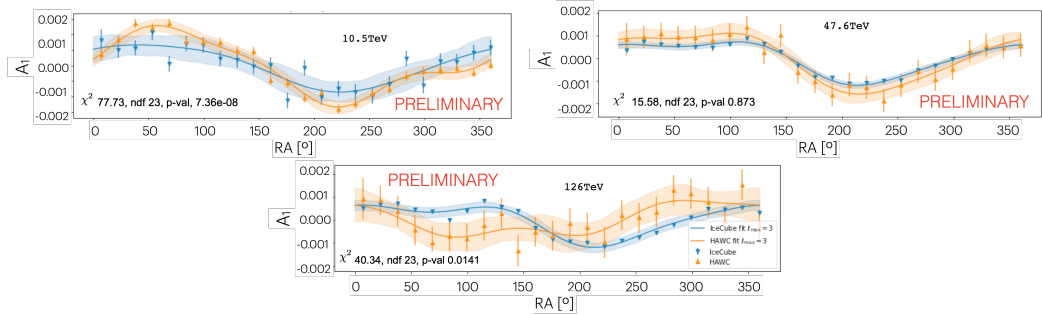


Figure 1: One-dimensional projection of relative intensity in the overlapping field of view of IceCube and HAWC. At 48 TeV energies, there is good statistical agreement between both experiments (top right). However at lower and higher energies (top left and center bottom), the two distributions are not statistically compatible.

5. Combined Anisotropy with IceCube

The overlapping FoV between the two observatories serves as a calibration region. Fig. 1 shows a one-dimensional projection of the relative intensity as a function of R.A. At 10 TeV energy, the distributions are qualitatively different but are statistically compatible. At 48 TeV energies, there is good agreement between both experiments. At 126 TeV, the distributions are not statistically compatible. According to the simulations, the cosmic-ray energy distribution in each bin should be comparable, however, the mass composition in each of the samples shown in Fig. 2, indicates that the two detectors have very different sensitivities to each of the mass groups. IceCube data appears to be dominated by protons and light elements at lower energies than HAWC but becomes heavier at ~ 150 TeV.

If we assume that the distribution of arrival directions of cosmic rays is rigidity-dependent rather than energy-dependent, we can compare the one-dimensional distributions for IceCube and HAWC at comparable rigidities and using a χ^2 test and assess whether we achieve better agreement. In order to find the optimal IceCube energy cuts to match the rigidity for each HAWC bin, we perform a scan and use a Kolmogorov-Smirnov test to compare the rigidity distributions assuming the GSF [16] composition model, as shown in Fig 2. Table 1 shows the median energies and

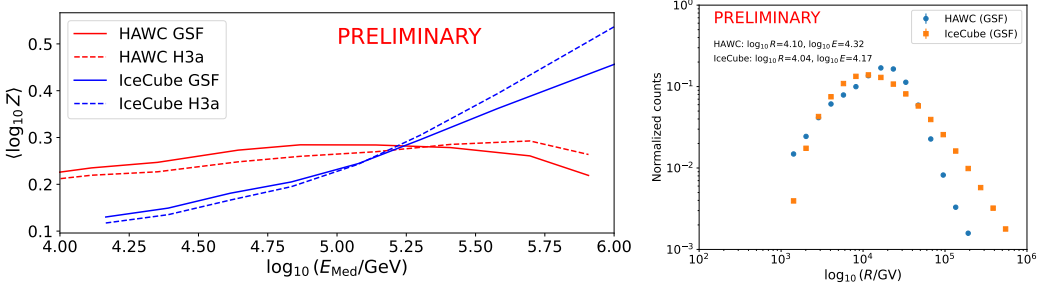


Figure 2: Left: mean logarithm of the particle charge Z for cosmic rays detected by IceCube (blue) and HAWC (red) assuming the Gaisser H3a [15] (dashed) and GSF [16] (solid) composition models. IceCube data is dominated by protons and light elements at lower energies than HAWC, but becomes heavier above about 200 TeV. Right: Assuming a rigidity-dependent angular distribution of cosmic rays, we find the most compatible energy bins (top) by sliding an IceCube energy window of size $\Delta \log_{10} E = 0.25$ and minimizing the KS test value between rigidity distributions based on Monte Carlo simulations.

rigidity for each bin. The combined IceCube–HAWC maps are shown in relative intensity (Fig. 3) and significance (Fig. 4) for seven rigidity-driven pairs of energy bins. The smoothing radius and thresholds are adjusted for higher energy bins to compensate for the decreasing statistics. A rapid phase transition is observed going from 40 TV to 76 TV consistent with previous individual measurements [1].

5.1 Angular Power Spectrum

The angular power spectrum (APS) defined as

$$C_\ell = \frac{1}{2\ell + 1} \sum_{m=-\ell}^{\ell} |a_{\ell m}|^2 , \quad (5)$$

for each value of ℓ , provides an estimate of the significance of structures at different angular scales of $\sim 180^\circ/\ell$. In case of full 4π sky coverage, the multipole moments $a_{\ell m}$ would give complete representation of the anisotropy. However, partial sky coverage results in large correlations between coefficients $a_{\ell m}$, biasing results. Fig. 5 shows the pseudo-angular power spectrum for all 11 HAWC rigidity maps. For maps above 4.1 TV, where we have IceCube–HAWC combined data, we include the combined angular power spectrum shown in red. The dipole power of the combined map is consistently larger than in the HAWC-only measurement, as some power is redistributed to higher C_ℓ terms due to correlations in the $a_{\ell m}$ coefficients. The isotropic noise level is driven by the region with the lowest statistics. In general, the APS has most power distributed to lower ℓ harmonics, corresponding to larger angular structures (e.g., dipole, quadrupole, etc.) and decreases for larger ℓ to be drowned in noise. In the case of combined maps, the noise level shown is computed from the total combined dataset. In some cases, the noise level of the combined maps is lower due to the increased statistics in the overlapping FoV.

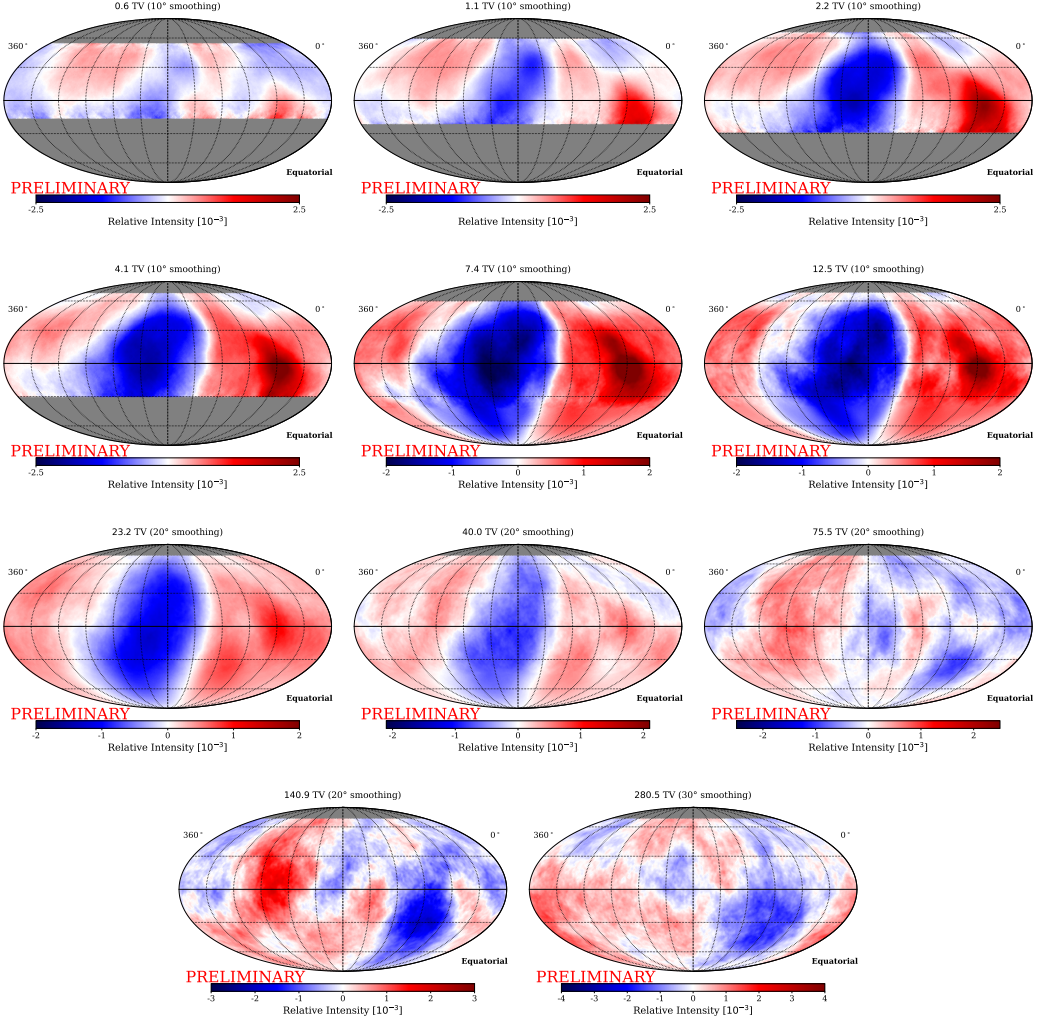


Figure 3: Relative intensity for 11 HAWC energy bins. Table 1 shows the median energies corresponding to each bin. The last seven maps correspond to rigidity-matching pairs of energy bins. Combined relative intensity maps are reconstructed using the maximum likelihood method of Ahlers et al. [13]. A rapid phase transition is observed going from 40 TV to 76 TV, consistent with previous individual measurements.

6. Conclusions and Outlook

We have presented preliminary results on an updated full-sky analysis of the cosmic-ray arrival direction distribution with data collected by the HAWC and IceCube observatories with complementary field of views jointly covering nearly 4π steradians. With 8 years of data, HAWC can extend the energy range from previous results [17] to higher energies. We include updated measurements by HAWC in the energy range between 3.0 TeV and 0.5 PeV, confirming previous results of an energy-dependent anisotropy in the arrival direction distribution of cosmic rays seen by other experiments. This analysis – which includes recently published results from IceCube with 12 years of data – is the first all-sky anisotropy study with primary cosmic-ray energies above 10 TeV. The combined maps and their corresponding angular power spectra largely eliminate biases

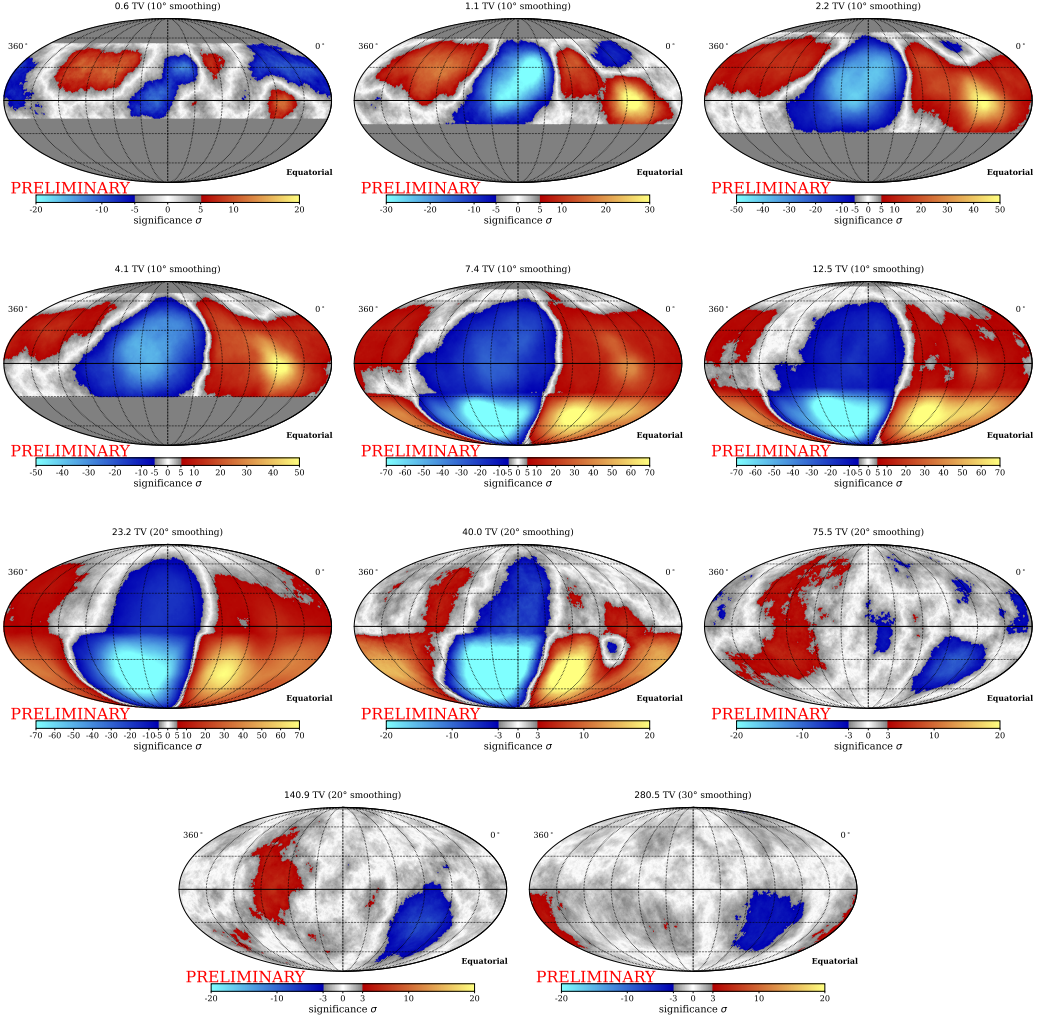


Figure 4: Li–Ma significance for 11 HAWC energy bins. Table 1 shows the median energies corresponding to each bin. The last seven maps correspond to rigidity-matching pairs of energy bins. Smoothing radius and thresholds are adjusted for higher energy bins to compensate for decreasing statistics.

that result from partial sky coverage. IceCube angular structures appear to evolve faster as a function of energy than they do for HAWC maps. Monte Carlo studies suggest that the angular distributions depend on rigidity rather than energy. The best-matching energy bins are consistent with this hypothesis. Further investigation is needed, including systematic studies that account for uncertainties in cosmic-ray composition models. We also need to extend this study by including data from other cosmic-ray observatories in both hemispheres that extend to higher and lower energies. Some of this work is already underway through various other collaborations.

References

- [1] R. Abbasi, M. Ackermann, J. Adams, *et al.*, *Astrophys. J.* **981** no. 2, (Mar, 2025) 182.
- [2] P. Sommers, *Astropart. Phys.* **14** no. 4, (2001) 271 – 286.

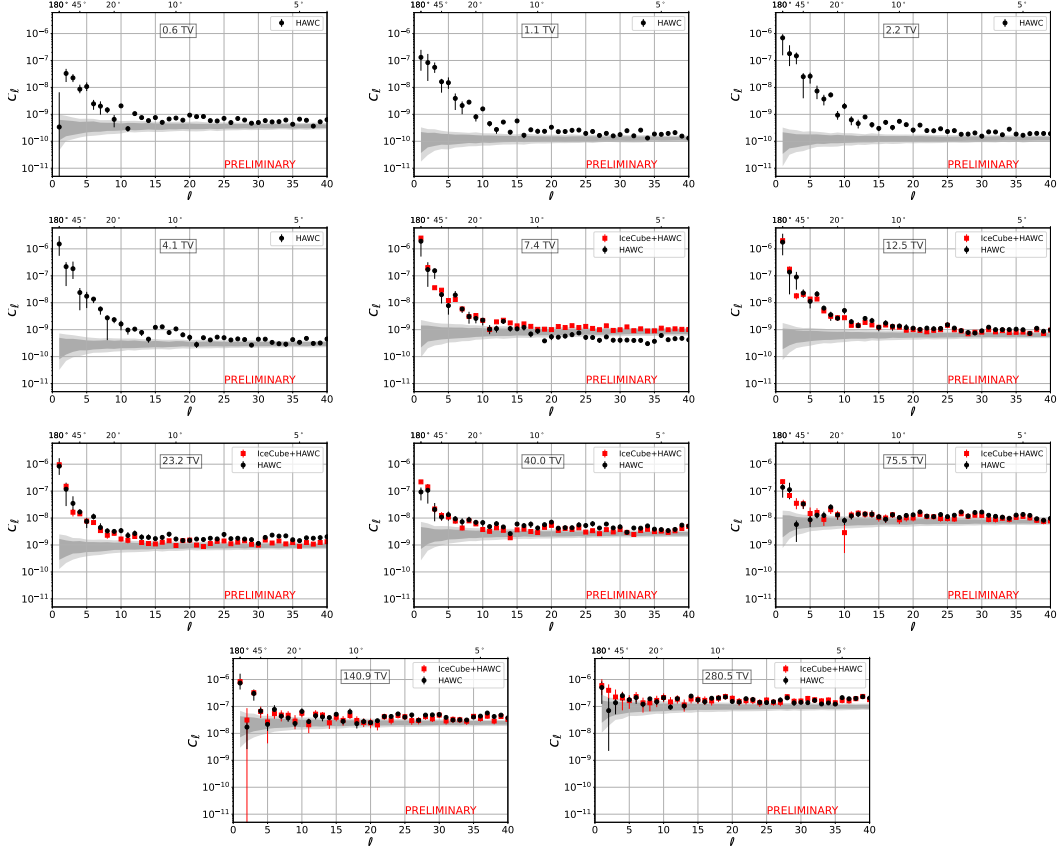


Figure 5: Angular power spectra for 11 HAWC sky maps binned in energy (black circles) and 7 combined all-sky IceCube+HAWC maps using rigidity-driven pairs of energy bins (red squares). Error bars represent statistical uncertainties. The shaded regions correspond to the isotropic noise at 68% (dark) and 90% (light) confidence intervals.

- [3] M. Ahlers, *ApJL* **886** no. 1, (Nov, 2019) L18.
- [4] **IceCube** Collaboration, M. G. Aartsen *et al.*, *JINST* **12** no. 03, (2017) P03012.
- [5] A. Abeysekara, A. Albert, R. Alfaro, *et al.*, *NIMPA* **1052** (2023) 168253.
- [6] N. Whitehorn *et al.*, *Comp. Phys. Com.* **184** no. 9, (2013) 2214 – 2220.
- [7] M. G. Aartsen *et al.*, *Astrophys. J.* **826** (Aug., 2016) 220.
- [8] S. Verpoest, D. Soldin, and P. Desiati, *Astropart. Phys.* **161** (2024) 102985.
- [9] A. H. Compton and I. A. Getting, *Phys. Rev.* **47** (Jun, 1935) 817–821.
- [10] T. Jenness and D. S. Berry, “PAL: A Positional Astronomy Library,” in *Astro. Data Analysis Software and Systems XXII*, D. N. Friedel, ed., vol. 475 of *ASP Conf. Series*, p. 307. 2013.
- [11] J. A. Morales-Soto and J. C. Arteaga-Velázquez, *PoS ICRC2023* (2023) 364.
- [12] K. M. Górski *et al.*, *Astrophys. J.* **622** (2005) 759–771.
- [13] M. Ahlers *et al.*, *Astrophys. J.* **823** no. 1, (2016) 10.
- [14] T. P. Li and Y. Q. Ma, *Astrophys. J.* **272** (1983) 317–324.
- [15] T. K. Gaisser, *Astropart. Phys.* **35** (2012) 801–806.
- [16] H. Dembinski, R. Engel, A. Fedynitch, *et al.*, *PoS ICRC2017* (2017) 533.
- [17] A. U. Abeysekara *et al.*, *Astrophys. J.* **865** no. 1, (2018) 57.

Full Author List: HAWC Collaboration

R. Alfaro¹, C. Alvarez², A. Andrés³, E. Anita-Rangel³, M. Araya⁴, J.C. Arteaga-Velázquez⁵, D. Avila Rojas³, H.A. Ayala Solares⁶, R. Babu⁷, P. Bangale⁸, E. Belmont-Moreno¹, A. Bernal³, K.S. Caballero-Mora², T. Capistrán⁹, A. Carramiñana¹⁰, F. Carreón³, S. Casanova¹¹, S. Coutiño de León¹², E. De la Fuente¹³, D. Depaoli¹⁴, P. Desiati¹², N. Di Lalla¹⁵, R. Diaz Hernandez¹⁰, B.L. Dingus¹⁶, M.A. DuVernois¹², J.C. Díaz-Vélez¹², K. Engel¹⁷, T. Ergin⁷, C. Espinoza¹, K. Fang¹², N. Fraija³, S. Fraija³, J.A. García-González¹⁸, F. Garfias³, N. Ghosh¹⁹, A. Gonzalez Muñoz¹, M.M. González³, J.A. Goodman¹⁷, S. Groetsch¹⁹, J. Gyeong²⁰, J.P. Harding¹⁶, S. Hernández-Cadena²¹, I. Herzog⁷, D. Huang¹⁷, P. Hüntemeyer¹⁹, A. Iriarte³, S. Kaufmann²², D. Kieda²³, K. Leavitt¹⁹, H. León Vargas¹, J.T. Linnemann⁷, A.L. Longinotti³, G. Luis-Raya²², K. Malone¹⁶, O. Martinez²⁴, J. Martínez-Castro²⁵, H. Martínez-Huerta³⁰, J.A. Matthews²⁶, P. Miranda-Romagnoli²⁷, P.E. Mirón-Enriquez³, J.A. Montes³, J.A. Morales-Soto⁵, M. Mostafá⁸, M. Najaf¹⁹, L. Nellen²⁸, M.U. Nisa⁷, N. Omodei¹⁵, E. Ponce²⁴, Y. Pérez Araujo¹, E.G. Pérez-Pérez²², Q. Remy¹⁴, C.D. Rho²⁰, D. Rosa-González¹⁰, M. Roth¹⁶, H. Salazar²⁴, D. Salazar-Gallegos⁷, A. Sandoval¹, M. Schneider¹, G. Schwefer¹⁴, J. Serna-Franco¹, A.J. Smith¹⁷, Y. Son²⁹, R.W. Springer²³, O. Tibolla²², K. Tollefson⁷, I. Torres¹⁰, R. Torres-Escobedo²¹, R. Turner¹⁹, E. Varela²⁴, L. Villaseñor²⁴, X. Wang¹⁹, Z. Wang¹⁷, I.J. Watson²⁹, H. Wu¹², S. Yu⁶, S. Yun-Cárcamo¹⁷, H. Zhou²¹,

¹Instituto de Física, Universidad Nacional Autónoma de México, Ciudad de Mexico, Mexico, ²Universidad Autónoma de Chiapas, Tuxtla Gutiérrez, Chiapas, México, ³Instituto de Astronomía, Universidad Nacional Autónoma de México, Ciudad de Mexico, Mexico, ⁴Universidad de Costa Rica, San José 2060, Costa Rica, ⁵Universidad Michoacana de San Nicolás de Hidalgo, Morelia, Mexico, ⁶Department of Physics, Pennsylvania State University, University Park, PA, USA, ⁷Department of Physics and Astronomy, Michigan State University, East Lansing, MI, USA, ⁸Temple University, Department of Physics, 1925 N. 12th Street, Philadelphia, PA 19122, USA, ⁹Università degli Studi di Torino, I-10125 Torino, Italy, ¹⁰Instituto Nacional de Astrofísica, Óptica y Electrónica, Puebla, Mexico, ¹¹Institute of Nuclear Physics Polish Academy of Sciences, PL-31342 11, Krakow, Poland, ¹²Dept. of Physics and Wisconsin IceCube Particle Astrophysics Center, University of Wisconsin—Madison, Madison, WI, USA, ¹³Departamento de Física, Centro Universitario de Ciencias Exactas Ingenierías, Universidad de Guadalajara, Guadalajara, Mexico, ¹⁴Max-Planck Institute for Nuclear Physics, 69117 Heidelberg, Germany, ¹⁵Department of Physics, Stanford University: Stanford, CA 94305–4060, USA, ¹⁶Los Alamos National Laboratory, Los Alamos, NM, USA, ¹⁷Department of Physics, University of Maryland, College Park, MD, USA, ¹⁸Tecnológico de Monterrey, Escuela de Ingeniería y Ciencias, Ave. Eugenio Garza Sada 2501, Monterrey, N.L., Mexico, 64849, ¹⁹Department of Physics, Michigan Technological University, Houghton, MI, USA, ²⁰Department of Physics, Sungkyunkwan University, Suwon 16419, South Korea, ²¹Tsung-Dao Lee Institute & School of Physics and Astronomy, Shanghai Jiao Tong University, 800 Dongchuan Rd, Shanghai, SH 200240, China, ²²Universidad Politécnica de Pachuca, Pachuca, Hgo, Mexico, ²³Department of Physics and Astronomy, University of Utah, Salt Lake City, UT, USA, ²⁴Facultad de Ciencias Físico Matemáticas, Benemérita Universidad Autónoma de Puebla, Puebla, Mexico, ²⁵Centro de Investigación en Computación, Instituto Politécnico Nacional, México City, México, ²⁶Dept of Physics and Astronomy, University of New Mexico, Albuquerque, NM, USA, ²⁷Universidad Autónoma del Estado de Hidalgo, Pachuca, Mexico, ²⁸Instituto de Ciencias Nucleares, Universidad Nacional Autónoma de Mexico, Ciudad de Mexico, Mexico, ²⁹University of Seoul, Seoul, Rep. of Korea, ³⁰Departamento de Física y Matemáticas, Universidad de Monterrey, Av. Morones Prieto 4500, 66238, San Pedro Garza García NL, México

Acknowledgments

We acknowledge the support from: the US National Science Foundation (NSF); the US Department of Energy Office of High-Energy Physics; the Laboratory Directed Research and Development (LDRD) program of Los Alamos National Laboratory; Consejo Nacional de Ciencia y Tecnología (CONACyT), México, grants LNC-2023-117, 271051, 232656, 260378, 179588, 254964, 258865, 243290, 132197, A1-S-46288, A1-S-22784, CF-2023-I-645, CBF2023-2024-1630, cátedras 873, 1563, 341, 323, Red HAWC, México; DGAPA-UNAM grants IG101323, IN1111716-3, IN111419, IA102019, IN106521, IN114924, IN110521, IN102223; VIEP-BUAP; PIFI 2012, 2013, PROFOCIE 2014, 2015; the University of Wisconsin Alumni Research Foundation; the Institute of Geophysics, Planetary Physics, and Signatures at Los Alamos National Laboratory; Polish Science Centre grant, 2024/53/B/ST9/02671; Coordinación de la Investigación Científica de la Universidad Michoacana; Royal Society - Newton Advanced Fellowship 180385; Gobierno de España and European Union-NextGenerationEU, grant CNS2023- 144099; The Program Management Unit for Human Resources & Institutional Development, Research and Innovation, NXPO (grant number B16F630069); Coordinación General Académica e Innovación (CGAI-UdeG), PRODEP-SEP UDG-CA-499; Institute of Cosmic Ray Research (ICRR), University of Tokyo. H.F. acknowledges support by NASA under award number 80GSFC21M0002. C.R. acknowledges support from National Research Foundation of Korea (RS-2023-00280210). We also acknowledge the significant contributions over many years of Stefan Westerhoff, Gaurang Yodh and Arnulfo Zepeda Domínguez, all deceased members of the HAWC collaboration. Thanks to Scott Delay, Luciano Díaz and Eduardo Murrieta for technical support.

Full Author List: IceCube Collaboration

R. Abbasi¹⁶, M. Ackermann⁶³, J. Adams¹⁷, S. K. Agarwalla^{39, a}, J. A. Aguilar¹⁰, M. Ahlers²¹, J.M. Alameddine²², S. Ali³⁵, N. M. Amin⁴³, K. Andeen⁴¹, C. Argüelles¹³, Y. Ashida⁵², S. Athanasiadou⁶³, S. N. Axani⁴³, R. Babu²³, X. Bai⁴⁹, J. Baines-Holmes³⁹, A. Balagopal V.^{39, 43}, S. W. Barwick²⁹, S. Bash²⁶, V. Basu⁵², R. Bay⁶, J. J. Beatty^{19, 20}, J. Becker Tjus^{9, b}, P. Behrens¹, J. Beise⁶¹, C. Bellenghi²⁶, B. Benkel⁶³, S. BenZvi⁵¹, D. Berley¹⁸, E. Bernardini^{47, c}, D. Z. Besson³⁵, E. Blaufuss¹⁸, L. Bloom⁵⁸, S. Blot⁶³, I. Bodo³⁹, F. Bontempo³⁰, J. Y. Book Motzkin¹³, C. Boscolo Meneguolo^{47, c}, S. Böser⁴⁰, O. Botner⁶¹, J. Böttcher¹, J. Braun³⁹, B. Brinson⁴, Z. Brisson-Tsavoussi³², R. T. Burley², D. Butterfield³⁹, M. A. Campana⁴⁸, K. Carloni¹³, J. Carpio^{33, 34}, S. Chattopadhyay^{39, a}, N. Chau¹⁰, Z. Chen⁵⁵, D. Chirkin³⁹, S. Choi⁵², B. A. Clark¹⁸, A. Coleman⁶¹, P. Coleman¹, G. H. Collin¹⁴, D. A. Coloma Borja⁴⁷, A. Connolly^{19, 20}, J. M. Conrad¹⁴, R. Corley⁵², D. F. Cowen^{59, 60}, C. De Clercq¹¹, J. J. DeLaunay⁵⁹, D. Delgado¹³, T. Delmeulle¹⁰, S. Deng¹, P. Desiati³⁹, K. D. de Vries¹¹, G. de Wasseige³⁶, T. DeYoung²³, J. C. Díaz-Vélez³⁹, S. DiKerby²³, M. Dittmer⁴², A. Domí²⁵, L. Draper⁵², L. Dueser¹, D. Durnford²⁴, K. Dutta⁴⁰, M. A. DuVernois³⁹, T. Ehrhardt⁴⁰, L. Eidenschink²⁶, A. Eimer²⁵, P. Eller²⁶, E. Ellinger⁶², D. Elsässer²², R. Engel^{30, 31}, H. Erpenbeck³⁹, W. Esmail⁴², S. Eulig¹³, J. Evans¹⁸, P. A. Evenson⁴³, K. L. Fan¹⁸, K. Fang³⁹, K. Farrag¹⁵, A. R. Fazely⁵, A. Fedynitch⁵⁷, N. Feigl⁸, C. Finley⁵⁴, L. Fischer⁶³, D. Fox⁵⁹, A. Franckowiak⁹, S. Fukami⁶³, P. Fürst¹, J. Gallagher³⁸, E. Ganster¹, A. Garcia¹³, M. Garcia⁴³, G. Garg^{39, a}, E. Genton^{13, 36}, L. Gerhardt⁷, A. Ghadimi⁵⁸, C. Glaser⁶¹, T. Glüsenkamp⁶¹, J. G. Gonzalez⁴³, S. Goswami^{33, 34}, A. Granados²³, D. Grant¹², S. J. Gray¹⁸, S. Griffin³⁹, S. Griswold⁵¹, K. M. Groth²¹, D. Guevel³⁹, C. Günther¹, P. Gutjahr²², C. Ha⁵³, C. Haack²⁵, A. Hallgren⁶¹, L. Halve¹, F. Halzen³⁹, L. Hamacher¹, M. Ha Minh²⁶, M. Handt¹, K. Hanson³⁹, J. Hardin¹⁴, A. A. Harnisch²³, P. Hatch³², A. Haungs³⁰, J. Häußler¹, K. Helbing⁶², J. Hellrung⁹, B. Henke²³, L. Hennig²⁵, F. Henningsen¹², L. Heuermann¹, R. Hewett¹⁷, N. Heyer⁶¹, S. Hickford⁶², A. Hidvegi⁵⁴, C. Hill¹⁵, G. C. Hill², R. Hmaid¹⁵, K. D. Hoffman¹⁸, D. Hooper³⁹, S. Hori³⁹, K. Hoshina^{39, d}, M. Hostert¹³, W. Hou³⁰, T. Huber³⁰, K. Hultqvist⁵⁴, K. Hymon^{22, 57}, A. Ishihara¹⁵, W. Iwakiri¹⁵, M. Jacquart²¹, S. Jain³⁹, O. Janik²⁵, M. Jansson³⁶, M. Jeong⁵², M. Jin¹³, N. Kamp¹³, D. Kang³⁰, W. Kang⁴⁸, X. Kang⁴⁸, A. Kappes⁴², L. Kardum²², T. Karg⁶³, M. Karl²⁶, A. Karle³⁹, A. Katil²⁴, M. Kauer³⁹, J. L. Kelley³⁹, M. Khanal⁵², A. Khatee Zathul³⁹, A. Kheirandish^{33, 34}, H. Kimku⁵³, J. Kiryluk⁵⁵, C. Klein²⁵, S. R. Klein^{6, 7}, Y. Kobayashi¹⁵, A. Kochcocki²³, R. Koiral⁴³, H. Kolanoski⁸, T. Kontrimas²⁶, L. Köpke⁴⁰, C. Kopper²⁵, D. J. Koskinen²¹, P. Koundal⁴³, M. Kowalski^{8, 63}, T. Kozynets²¹, N. Krieger⁹, J. Krishnamoorthi^{39, a}, T. Krishnan¹³, K. Kruiswijk³⁶, E. Krupczak²³, A. Kumar⁶³, E. Kun⁹, N. Kurahashi⁴⁸, N. Lad⁶³, C. Lagunas Gualda²⁶, L. Lallement Arnaud¹⁰, M. Lamoureux³⁰, M. J. Larson¹⁸, F. Lauber⁶², J. P. Lazar³⁶, K. Leonard DeHolton⁶⁰, A. Leszczyńska⁴³, J. Liao⁴, C. Lin⁴³, Y. T. Liu⁶⁰, M. Liubarska²⁴, C. Love⁴⁸, L. Lu³⁹, F. Lucarelli²⁷, W. Luszczak^{19, 20}, Y. Lyu^{6, 7}, J. Madsen³⁹, E. Magnus¹¹, K. B. M. Mahn²³, Y. Makino³⁹, E. Manao²⁶, S. Mancina^{47, e}, A. Mand³⁹, I. C. Maris¹⁰, S. Marka⁴⁵, Z. Marka⁴⁵, L. Marten¹, I. Martinez-Soler¹³, R. Maruyama⁴⁴, J. Mauro³⁶, F. Mayhew²³, F. McNally³⁷, J. V. Mead²¹, K. Meagher³⁹, S. Mechbal⁶³, A. Medina²⁰, M. Meier¹⁵, Y. Merckx¹¹, L. Merten⁹, J. Mitchell⁵, L. Molchany⁴⁹, T. Montaruli²⁷, R. W. Moore²⁴, Y. Morii¹⁵, A. Mosbrugger²⁵, M. Mouhai³⁹, D. Mousadi⁶³, E. Moyaux³⁶, T. Mukherjee³⁰, R. Naab⁶³, M. Nakos³⁹, U. Naumann⁶², J. Necker⁶³, L. Neste⁵⁴, M. Neumann⁴², H. Niederhausen²³, M. U. Nisa²³, K. Noda¹⁵, A. Noell¹, A. Novikov⁴³, A. Obertacke Pollmann¹⁵, V. O'Dell³⁹, A. Olivas¹⁸, R. Orsoe²⁶, J. Osborn³⁹, E. O'Sullivan⁶¹, V. Palusova⁴⁰, H. Pandya⁴³, A. Parenti¹⁰, N. Park³², V. Parrish²³, E. N. Paudel⁵⁸, L. Paul⁴⁹, C. Pérez de los Heros⁶¹, T. Pernice⁶³, J. Peterson³⁹, M. Plum⁴⁹, A. Pontén⁶¹, V. Poojyam⁵⁸, Y. Popovich⁴⁰, M. Prado Rodriguez³⁹, B. Pries²³, R. Procter-Murphy¹⁸, G. T. Przybyski⁷, L. Pyras⁵², C. Raab³⁶, J. Rack-Helleis⁴⁰, N. Rad⁶³, M. Ravn⁶¹, K. Rawlins³, Z. Rechav³⁹, A. Rehman⁴³, I. Reistroffer⁴⁹, E. Resconi²⁶, S. Reusch⁶³, C. D. Rho⁵⁶, W. Rhode²², L. Ricca³⁶, B. Riedel³⁹, A. Rifaiet⁶², E. J. Roberts², S. Robertson^{6, 7}, M. Rongen²⁵, A. Rosted¹⁵, C. Rott⁵², T. Ruhe²², L. Ruohan²⁶, D. Ryckbosch²⁸, J. Saffer³¹, D. Salazar-Gallegos²³, P. Sampathkumar³⁰, A. Sandrock⁶², G. Sanger-Johnson²³, M. Santander⁵⁸, S. Sarkar⁴⁶, J. Savelberg¹, M. Scarnera³⁶, P. Schaile²⁶, M. Schaufel¹, H. Schieles³⁰, S. Schindler²⁵, L. Schlückmann⁴⁰, B. Schlüter⁴², F. Schlüter¹⁰, N. Schmeisser⁶², T. Schmidt¹⁸, F. G. Schröder^{30, 43}, L. Schumacher²⁵, S. Schwirn¹, S. Scalfani¹⁸, D. Seckel⁴³, L. Seen³⁹, M. Seikh³⁵, S. Seunarine⁵⁰, P. A. Sevle Myhr³⁶, R. Shah⁴⁸, S. Shefali³¹, N. Shimizu¹⁵, B. Skrzypek⁶, R. Snihur³⁹, J. Soedingrekso²², A. Søgaard²¹, D. Soldin⁵², P. Soldin¹, G. Sommani⁹, C. Spannfellner²⁶, G. M. Spiczak⁵⁰, C. Spiering⁶³, J. Stachurska²⁸, M. Stamatikos²⁰, T. Staney⁴³, T. Stezelberger⁷, T. Stürwald⁶², T. Stuttard²¹, G. W. Sullivan¹⁸, I. Taboada⁴, S. Ter-Antonyan⁵, A. Terliuk²⁶, A. Thakuri⁴⁹, M. Thiesmeyer³⁹, W. G. Thompson¹³, J. Thwaites³⁹, S. Tilay⁴³, K. Tollefson²³, S. Toscano¹⁰, D. Tosi³⁹, A. Trettin⁶³, A. K. Upadhyay^{39, a}, K. Upshaw⁵, A. Vaidyanathan⁴¹, N. Valtonen-Mattila^{9, 61}, J. Valverde⁴¹, J. Vandembroucke³⁹, T. van Eeden⁶³, N. van Eijndhoven¹¹, L. van Rootselaar²², J. van Santen⁶³, F. J. Vara Carbonell⁴², F. Varsi³¹, M. Venugopal³⁰, M. Vereecken³⁶, S. Vergara Carrasco¹⁷, S. Verpoest⁴³, D. Veske⁴⁵, A. Vijai¹⁸, J. Villarreal¹⁴, C. Walck⁵⁴, A. Wang⁴, E. Warrick⁵⁸, C. Weaver²³, P. Weigel¹⁴, A. Weindl³⁰, J. Weldert⁴⁰, A. Y. Wen¹³, C. Wendt³⁹, J. Werthebach²², M. Weyrauch³⁰, N. Whitehorn²³, C. H. Wiebusch¹, D. R. Williams⁵⁸, L. Witthaus²², M. Wolf²⁶, G. Wrede²⁵, X. W. Xu⁵, J. P. Yanéz²⁴, Y. Yao³⁹, E. Yildizci³⁹, S. Yoshida¹⁵, R. Young³⁵, F. Yu¹³, S. Yu⁵², T. Yuan³⁹, A. Zegarelli⁹, S. Zhang²³, Z. Zhang⁵⁵, P. Zilberman³⁹

¹ III. Physikalisches Institut, RWTH Aachen University, D-52056 Aachen, Germany

² Department of Physics, University of Adelaide, Adelaide, 5005, Australia

³ Dept. of Physics and Astronomy, University of Alaska Anchorage, 3211 Providence Dr., Anchorage, AK 99508, USA

⁴ School of Physics and Center for Relativistic Astrophysics, Georgia Institute of Technology, Atlanta, GA 30332, USA

⁵ Dept. of Physics, Southern University, Baton Rouge, LA 70813, USA

⁶ Dept. of Physics, University of California, Berkeley, CA 94720, USA

⁷ Lawrence Berkeley National Laboratory, Berkeley, CA 94720, USA

⁸ Institut für Physik, Humboldt-Universität zu Berlin, D-12489 Berlin, Germany

⁹ Fakultät für Physik & Astronomie, Ruhr-Universität Bochum, D-44780 Bochum, Germany

¹⁰ Université Libre de Bruxelles, Science Faculty CP230, B-1050 Brussels, Belgium

- ¹¹ Vrije Universiteit Brussel (VUB), Dienst ELEM, B-1050 Brussels, Belgium
¹² Dept. of Physics, Simon Fraser University, Burnaby, BC V5A 1S6, Canada
¹³ Department of Physics and Laboratory for Particle Physics and Cosmology, Harvard University, Cambridge, MA 02138, USA
¹⁴ Dept. of Physics, Massachusetts Institute of Technology, Cambridge, MA 02139, USA
¹⁵ Dept. of Physics and The International Center for Hadron Astrophysics, Chiba University, Chiba 263-8522, Japan
¹⁶ Department of Physics, Loyola University Chicago, Chicago, IL 60660, USA
¹⁷ Dept. of Physics and Astronomy, University of Canterbury, Private Bag 4800, Christchurch, New Zealand
¹⁸ Dept. of Physics, University of Maryland, College Park, MD 20742, USA
¹⁹ Dept. of Astronomy, Ohio State University, Columbus, OH 43210, USA
²⁰ Dept. of Physics and Center for Cosmology and Astro-Particle Physics, Ohio State University, Columbus, OH 43210, USA
²¹ Niels Bohr Institute, University of Copenhagen, DK-2100 Copenhagen, Denmark
²² Dept. of Physics, TU Dortmund University, D-44221 Dortmund, Germany
²³ Dept. of Physics and Astronomy, Michigan State University, East Lansing, MI 48824, USA
²⁴ Dept. of Physics, University of Alberta, Edmonton, Alberta, T6G 2E1, Canada
²⁵ Erlangen Centre for Astroparticle Physics, Friedrich-Alexander-Universität Erlangen-Nürnberg, D-91058 Erlangen, Germany
²⁶ Physik-department, Technische Universität München, D-85748 Garching, Germany
²⁷ Département de physique nucléaire et corpusculaire, Université de Genève, CH-1211 Genève, Switzerland
²⁸ Dept. of Physics and Astronomy, University of Gent, B-9000 Gent, Belgium
²⁹ Dept. of Physics and Astronomy, University of California, Irvine, CA 92697, USA
³⁰ Karlsruhe Institute of Technology, Institute for Astroparticle Physics, D-76021 Karlsruhe, Germany
³¹ Karlsruhe Institute of Technology, Institute of Experimental Particle Physics, D-76021 Karlsruhe, Germany
³² Dept. of Physics, Engineering Physics, and Astronomy, Queen's University, Kingston, ON K7L 3N6, Canada
³³ Department of Physics & Astronomy, University of Nevada, Las Vegas, NV 89154, USA
³⁴ Nevada Center for Astrophysics, University of Nevada, Las Vegas, NV 89154, USA
³⁵ Dept. of Physics and Astronomy, University of Kansas, Lawrence, KS 66045, USA
³⁶ Centre for Cosmology, Particle Physics and Phenomenology - CP3, Université catholique de Louvain, Louvain-la-Neuve, Belgium
³⁷ Department of Physics, Mercer University, Macon, GA 31207-0001, USA
³⁸ Dept. of Astronomy, University of Wisconsin—Madison, Madison, WI 53706, USA
³⁹ Dept. of Physics and Wisconsin IceCube Particle Astrophysics Center, University of Wisconsin—Madison, Madison, WI 53706, USA
⁴⁰ Institute of Physics, University of Mainz, Staudinger Weg 7, D-55099 Mainz, Germany
⁴¹ Department of Physics, Marquette University, Milwaukee, WI 53201, USA
⁴² Institut für Kernphysik, Universität Münster, D-48149 Münster, Germany
⁴³ Bartol Research Institute and Dept. of Physics and Astronomy, University of Delaware, Newark, DE 19716, USA
⁴⁴ Dept. of Physics, Yale University, New Haven, CT 06520, USA
⁴⁵ Columbia Astrophysics and Nevis Laboratories, Columbia University, New York, NY 10027, USA
⁴⁶ Dept. of Physics, University of Oxford, Parks Road, Oxford OX1 3PU, United Kingdom
⁴⁷ Dipartimento di Fisica e Astronomia Galileo Galilei, Università Degli Studi di Padova, I-35122 Padova PD, Italy
⁴⁸ Dept. of Physics, Drexel University, 3141 Chestnut Street, Philadelphia, PA 19104, USA
⁴⁹ Physics Department, South Dakota School of Mines and Technology, Rapid City, SD 57701, USA
⁵⁰ Dept. of Physics, University of Wisconsin, River Falls, WI 54022, USA
⁵¹ Dept. of Physics and Astronomy, University of Rochester, Rochester, NY 14627, USA
⁵² Department of Physics and Astronomy, University of Utah, Salt Lake City, UT 84112, USA
⁵³ Dept. of Physics, Chung-Ang University, Seoul 06974, Republic of Korea
⁵⁴ Oskar Klein Centre and Dept. of Physics, Stockholm University, SE-10691 Stockholm, Sweden
⁵⁵ Dept. of Physics and Astronomy, Stony Brook University, Stony Brook, NY 11794-3800, USA
⁵⁶ Dept. of Physics, Sungkyunkwan University, Suwon 16419, Republic of Korea
⁵⁷ Institute of Physics, Academia Sinica, Taipei, 11529, Taiwan
⁵⁸ Dept. of Physics and Astronomy, University of Alabama, Tuscaloosa, AL 35487, USA
⁵⁹ Dept. of Astronomy and Astrophysics, Pennsylvania State University, University Park, PA 16802, USA
⁶⁰ Dept. of Physics, Pennsylvania State University, University Park, PA 16802, USA
⁶¹ Dept. of Physics and Astronomy, Uppsala University, Box 516, SE-75120 Uppsala, Sweden
⁶² Dept. of Physics, University of Wuppertal, D-42119 Wuppertal, Germany
⁶³ Deutsches Elektronen-Synchrotron DESY, Platanenallee 6, D-15738 Zeuthen, Germany
^a also at Institute of Physics, Sachivalaya Marg, Sainik School Post, Bhubaneswar 751005, India
^b also at Department of Space, Earth and Environment, Chalmers University of Technology, 412 96 Gothenburg, Sweden
^c also at INFN Padova, I-35131 Padova, Italy
^d also at Earthquake Research Institute, University of Tokyo, Bunkyo, Tokyo 113-0032, Japan
^e now at INFN Padova, I-35131 Padova, Italy

Acknowledgments

The authors gratefully acknowledge the support from the following agencies and institutions: USA – U.S. National Science Foundation-Office of Polar Programs, U.S. National Science Foundation-Physics Division, U.S. National Science Foundation-EPSCoR, U.S. National Science Foundation-Office of Advanced Cyberinfrastructure, Wisconsin Alumni Research Foundation, Center for High Throughput Computing (CHTC) at the University of Wisconsin-Madison, Open Science Grid (OSG), Partnership to Advance Throughput Computing (PATh), Advanced Cyberinfrastructure Coordination Ecosystem: Services & Support (ACCESS), Frontera and Ranch computing project at the Texas Advanced Computing Center, U.S. Department of Energy-National Energy Research Scientific Computing Center, Particle astrophysics research computing center at the University of Maryland, Institute for Cyber-Enabled Research at Michigan State University, Astroparticle physics computational facility at Marquette University, NVIDIA Corporation, and Google Cloud Platform; Belgium – Funds for Scientific Research (FRS-FNRS and FWO), FWO Odysseus and Big Science programmes, and Belgian Federal Science Policy Office (Belspo); Germany – Bundesministerium für Forschung, Technologie und Raumfahrt (BMFTR), Deutsche Forschungsgemeinschaft (DFG), Helmholtz Alliance for Astroparticle Physics (HAP), Initiative and Networking Fund of the Helmholtz Association, Deutsches Elektronen Synchrotron (DESY), and High Performance Computing cluster of the RWTH Aachen; Sweden – Swedish Research Council, Swedish Polar Research Secretariat, Swedish National Infrastructure for Computing (SNIC), and Knut and Alice Wallenberg Foundation; European Union – EGI Advanced Computing for research; Australia – Australian Research Council; Canada – Natural Sciences and Engineering Research Council of Canada, Calcul Québec, Compute Ontario, Canada Foundation for Innovation, WestGrid, and Digital Research Alliance of Canada; Denmark – Villum Fonden, Carlsberg Foundation, and European Commission; New Zealand – Marsden Fund; Japan – Japan Society for Promotion of Science (JSPS) and Institute for Global Prominent Research (IGPR) of Chiba University; Korea – National Research Foundation of Korea (NRF); Switzerland – Swiss National Science Foundation (SNSF).